Acta Oceanol. Sin., 2016, Vol. 35, No. 1, P. 118–124
DOI: 10.1007/s13131-016-0803-3
http://www.hyxb.org.cn
E-mail: hyxbe@263.net

Further studies on the numerical simulation of bubble plumes in the cold seepage active region

LI Canping[1, 2], GOU Limin[3]*, YOU Jiachun[4], LIU Xuewei[4], OU Chuling[2]

[1] Guangdong Province Key Laboratory for Coastal Ocean Variation and Disaster Prediction (GLOD), Guangdong Ocean University, Zhanjiang 524088, China

[2] Laboratory of Ocean Remote Sensing and Information Technology, Guangdong Ocean University, Zhanjiang 524088, China

[3] School of Ocean Sciences, China University of Geosciences (Beijing), Beijing 100083, China

[4] School of Geophysics and Information Technology, China University of Geosciences (Beijing), Beijing 100083, China

Received 19 March 2015; accepted 8 September 2015

Abstract

Using the occurrence characteristics of bubble plumes in the South China Sea as a reference, this paper continues to study the seismic responses produced by bubble plumes in the cold seepage active region. To make the plume modelling scheme more reasonable, we modified the original modelling scheme and reconstructed a plume water body model based on the variation of its radius as bubbles rise in seawater. The plume seismic records of shot gathers were obtained by forward simulation. The seismic records of single shot show obvious characteristics of a scattering wave field and the periodic characteristics of the model. Seismic records of shot gathers were processed using prestack depth migration. The boundary of its imaging section has a good convergence effect. The migration sections can be imaged distinctly with higher accuracy. The aforementioned studies once again laid a foundation for the further study of the seismic responses produced by plumes. They also gradually probed a more suitable seismic data processing method for plumes and provided a theoretical guidance for the identification of plumes.

Key words: plume, cold seepage, gas hydrate, scattered wave, numerical simulation

Citation: Li Canping, Gou Limin, You Jiachun, Liu Xuewei, Ou Chuling. 2016. Further studies on the numerical simulation of bubble plumes in the cold seepage active region. Acta Oceanologica Sinica, 35(1): 118–124, doi: 10.1007/s13131-016-0803-3

1 Introduction

There is a large amount of global gas hydrate resources. The total amount of organic carbon contained in gas hydrates is estimated (Kvenvolden, 1993; Kvenvolden et al., 1993) to be equivalent to twice that in the known world coal, oil and natural gas reserves combined. The amount of gas hydrates in the sea account for more than 99% of the total amount (Fan et al., 2004). Therefore, natural gas hydrates have important energy and strategic significance, and the recognition, exploration and development of hydrates are a hotspot in current scientific research. In recent years, China has made some progress in hydrate exploration and exploitation (Wang et al., 2013; Hao et al., 2013; Lu et al., 2013; Zhang, 2010) and successfully drilled gas hydrate samples in the northern South China Sea on May 1, 2007. It is presumed that there are 27 regions of the China Sea where gas hydrates exist.

Cold seepage is a marine geological phenomenon that is caused by gases from seafloor (or deeper) sediments erupting into the ocean by expulsion and leakage (Di et al., 2008; Luan et al., 2010). One of the sources of hydrocarbon gases from seafloor cold seepage is methane dissociated from gas hydrates (Di et al., 2008). Hence, cold seepage may indicate the possible existence of gas hydrates beneath the seafloor. If the gas content of cold seepages is abundant, the gases may rise into the seawater and form a bubble plume. Therefore, a plume is a direct manifestation of seafloor seep activity, which has received an increasing amount of attention from scientists. One of the reasons for all of this attention is that the leakage type of natural gas hydrate precipitation is closely related to cold seepage activities, while on the other hand, the bubble plumes generated by seafloor seep activity are an important factor of the marine environment and the effect of global climate change, according to the expert opinion on the National Natural Fund of the first author in 2013.

It is estimated that more than 900 submarine seep activity areas exist in the global marine environment (Di et al., 2010; Tryon and Brown, 2004; MacDonalda et al., 2005; Tryon et al., 2002; Shipboard Scientific Party, 2002; Klaucke et al., 2010; Bayon et al., 2011). In addition, gas hydrates are commonly abundant in these areas. It is preliminarily confirmed that there are 7 cold seep areas offshore of China, and 6 of them are in the South China Sea, while only 1 of them is in the East China Sea (Luan et al., 2010). Many bubble plumes are found throughout the world (Sauter et al., 2006; Luan et al., 2010; Sassen et al., 2001; Gong, 2006; Freire et al., 2011; Charlou et al., 2003), and these areas are rich in gas hydrates. Plume bubbles carrying hydrates erupt from the seafloor and form a submarine "flame" phenomenon, and a 1 300-

Foundation item: The National Natural Science Foundation under contract No. 41306050; the Science and Technology Project of Guangdong Province under contract No. 2014A010103030; the Natural Science Foundation of Guangdong Province under contract No. 2015A030313617; the National Marine Important Charity Special Foundation under contract No. 201305019.

*Corresponding author, E-mail: goulm@163.com

m-high rising methane plume was discharged from a mud volcano in the Black Sea (Fig. 1) (Greinert et al., 2006).

From the above information, it is concluded that plumes are often found in cold seepage areas, while the two are related to gas hydrates.

At present, plumes are identified mostly through photography and sonar acoustic technology (Sassen et al., 2001; Sauter et al., 2006; Gong, 2006; Luan et al., 2010) that have a high image resolution, and the plumes are clear and visible. Because the scale of a plume bubbles is very small compared to the acoustic wavelength, according to the theory of seismic wave scattering (Wu and Aki, 1993), an acoustic wave will encounter scattering when it meets bubbles. Consequently, plumes can be recognized by imaging the water scattering in marine seismic data (Holbrook et al., 2003; Pinheiro et al., 2010).

Figure 2a is the seismic migration section of an area in the South China Sea, and there are special vent structures (a fault passes through the stratum and reaches seafloor), a typical Bottom Simulating Reflector (BSR) and a Blanking zone in the section. Figure 2b (Li et al., 2013) shows the conventional seismic

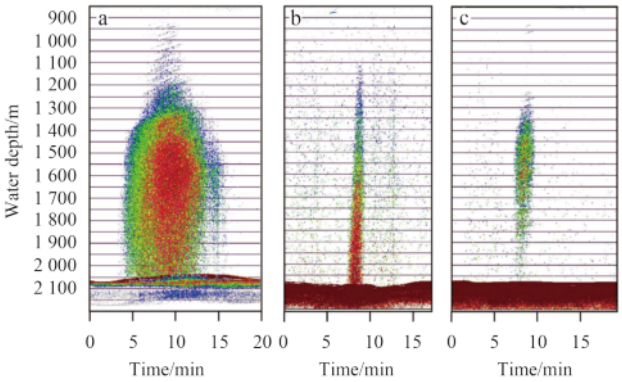

Fig. 1. The methane plume in the Black Sea.

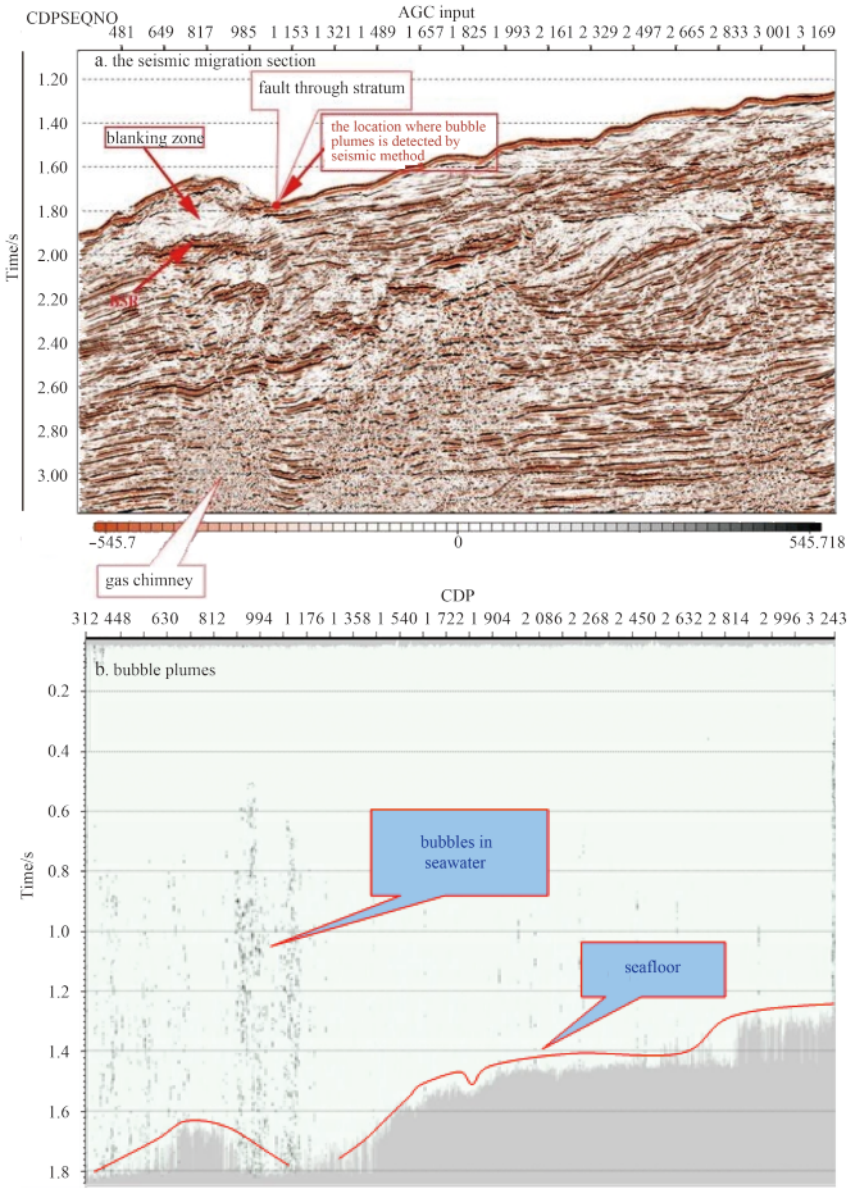

Fig. 2. The seismic migration section and bubble plumes of an area in the South China Sea.

migration section of seawater containing bubble plumes in the same area as Fig. 2a. Integrating the analyses of Figs 2a and b, this proof leads us to believe that the gas chimney and fault provides a channel to allow methane to spill into the sea, and the decomposition of gas hydrates is the source of the methane plumes. Therefore, the occurrence of methane plumes plays an indicative role in the gas hydrate exploration target area (Heeschen et al., 2003).

The above example shows that the seismic method can also be used to detect bubble plumes in seawater, and the seismicity is one of the main means of detecting bubble plumes on the regional scale. However, it does not form a complete set of method system for how to process seismic data to identify plumes, and at present, internationally, it is also inconclusive how the seismic response mechanism of plume behaves, according to the expert opinion on the National Natural Fund of the first author in 2013.

Therefore, in view of above problems, this subject will continue to carry out a numerical simulation of plumes.

2 The foundation of model building

2.1 *The features of a water body containing bubbles*

By consulting references, a water body containing bubbles has the following characteristics.

First, the experimental findings (Liu and Liu, 2010) are that when air is dissolved in water, the acoustic velocity of water will not change, even if the dissolved air reaches the saturation state. However, when air is not dissolved in water in the form of gas bubbles, the acoustic velocity of the water will be changed greatly, even with a small amount of air bubbles.

Second, small bubbles are more stable than large bubbles, bubbles in deep water are more stable than those in shallow water, and large and small bubbles show sequentially layered features at the moment the bubble rises (Xu and Liu, 2008).

Third, The experimental study and numerical simulation of the bubble rising velocity show (Ju et al., 2011) that the rising velocity of bubbles in still water is greater when the initial bubble radius is larger; when the initial bubble radius is smaller, the experienced time of reaching terminal velocity is shorter as the bubble rises in still water. The rate of change in the radius in the bubble rising process increases as the initial bubble radius and the rising speed of the bubbles increases.

Fourth, the acoustic velocity in the sea itself is vertically stratified (Liu and Liu, 2010) because three important factors (temperature, salinity and pressure) affecting the acoustic velocity of seawater vary with depth and are also vertically stratified. However, in seawater without bubbles, the change in the acoustic velocity due to the layer characteristics is lower and within approximately 30 m/s.

Fifth, the measured results (Hu et al., 2012) show that bubbles from hydrate decomposition, which rise to the sea, have little impact on the overall density of seawater.

Sixth, the actual detection results (Sauter et al., 2006) show that the plume bubble radius is mostly at the mm level, according to the seismic scattering theory (Wu and Aki, 1993), and bubbles in seawater will produce a scattering effect on seismic waves and generate a response in the seismic section.

The above conclusions not only provide evidences for the primary modelling idea and scheme but also provide a basis for the amendment of the original modelling scheme and the re-establishment of the plume model.

2.2 *Acoustic velocity of a water body containing bubbles*

The dissolved gas in the liquid and bubbles generated in the cavitation process will change the pressure distribution in the liquid (Liu and An, 2004), and thus, the acoustic characteristics of the liquid will also change. Taking the acoustic pressure of the bubble wall and the radial vibration velocity for boundary conditions, Yao Wenwei has deduced the following expression of the acoustic velocity in medium containing bubbles (Yao, 2008), as shown in Eq. (1):

$$C_{\mathrm{m}}{}^2 = \frac{K(3K_b - \rho\omega^2 a^2 - \frac{2\sigma}{a}) + \rho\omega^2 R^2 \phi(K - K_b + \frac{2\sigma}{3a})}{3K_b - \rho\omega^2 a^2 - \frac{2\sigma}{a} + 3\phi(K - K_b + \frac{2\sigma}{3a})} \times \frac{(\rho + 2\rho_b + \frac{4\sigma}{\omega^2 a^3}) + 2\phi(\rho - \rho_b - \frac{2\sigma}{\omega^2 a^3})}{\rho(\rho + 2\rho_b + \frac{4\sigma}{\omega^2 a^3}) - \phi\rho(\rho - \rho_b - \frac{2\sigma}{\omega^2 a^3})} . \quad (1)$$

In Eq. (1), the parameters K, K_{b}, ρ, ρ_{b} and σ are constant, while ω, a, ϕ and are variable. Thus, with the given parameters, the acoustic velocity of seawater that contains bubbles can be calculated by this formula as the bubble radius and content are varied.

Table 1 is a detailed description of the parameters in Eq. (1).

3 Improved water body model of the bubble plume

In the cold seepage active region, the plume phenomena result from bubbles produced by the leakage of methane gas into seawater. Plumes will change the pressure distribution and the acoustic properties of seawater. The acoustic velocities of seawater that contains bubbles are related to the bubble radius and content. The acoustic wave velocity of a bubble plume can be obtained using the acoustic velocity Eq. (1) in the medium with bubbles. Due to the random distribution of plume bubbles in seawater, the gas-liquid two-phase medium also belongs to the random medium. Therefore, we may construct the plume water body model based on the random medium theory and the acoustic wave velocity calculated from Eq. (1). This concept was discussed in reference (Li et al., 2013), and this paper will improve the modelling on this basis.

The bubble radius and content in the original plume model (the plume in reference (Li et al., 2013), the same below) first increase and then decrease throughout the 1 000-m depth range. In fact, the bubble to break up rising to 600 m. Through analysis on the reference conclusions in Section 2.1 of this paper, a relationship between the bubble rise velocity and bubble radius is obtained. According to the relationship, the following conclusions are drawn: a 0.5-mm radius bubble rising to 260 m may increase to 5 mm by further derivation, and the bubble will break up after

Table 1. The parameters in Eq. (1)

Parametric notation	Physical meaning of parameters	Values
C_{m}	acoustic velocity of gas-liquid mixture/m·s^{-1}	–
K	bulk modulus of liquid/N·m^{-3}	2.34×10^9
K_{b}	bulk modulus of gas/N·m^{-3}	1.4×10^5
ρ	density of liquid/kg·m^{-3}	1 023
ρ_{b}	density of gas/kg·m^{-3}	1.29
ω	frequency/kHz	25
a	bubble radius/m	–
σ	surface tension of liquid/N·m^{-3}	0.073 8
R	the radius of assuming the two phase mixing region containing the bubble is spherical/m	1.0
ϕ	bubble content (volume fraction)	–

it radius increases to 5 mm in seawater. Therefore, the bubble rises from 1 350 m below sea level to 350 m (the depth of the actual plume in Fig. 2b), and it is not possible for the radius to experience only an increase at first (increases to a certain extent and begins breaking up or cracking) followed by a decrease (the modelling idea of original plume).

Through the above analysis, the plume modelling scheme is modified as follows. The 1 000 m depth range of the original plume model is divided into three periods, and the bubble radius and content of each period increases first and then decreases. Taking into account the bubbles breaking into small air bubbles as they rise, the bubble radius will gradually decrease, so the depth range in the three periods is 420 m, 340 m and 240 m, respectively, from deep to shallow. The longitudinal change principle of the bubble radius and content in each period is the same in the original model. Namely, after a bubble rises to a certain height, the bubble begins to break up or split into smaller bubbles, resulting in a decrease in the bubble radii, while the content also decreases (the content is the volume content, so it will also decrease). The bubble radius and content in each layer of each period still change randomly around the bubble background radius and background content, and it is the same with the principle in reference (Li et al., 2013).

According to the above model modifying program, the plume model was re-established. To obtain better imaging results, the 250-m homogeneous layer (its speed is 1 520 m/s) was added at the bottom of original model, and it is equivalent to a uniform thin submarine layer. Finally, a water body model of the finished plume is shown in Fig. 3.

In Fig. 3, the plume water body model size is 3 500 m in the horizontal direction and 1 600 m in the longitudinal direction, and the grid is 1 m in the horizontal and longitudinal directions. The plume is in the middle of model, which is located in the range of 1 650 to 1 850 m and at a depth of 350–1 350 m in the longitudinal direction. The plume region is lateral 200 m and vertical 1 000 m, as is shown in Fig. 3b, and it is the magnified image of plume in the middle of Fig. 3a.

The background values of the bubble radius and content in the three periods (from shallow to deep order) are as follows in Fig. 3.

In the first period, the background radius ranges from 4.6×10^{-4} m to 4.6×10^{-3} m to 4.6×10^{-4} m, and the background content ranges from 1.8×10^{-6} to 4.6×10^{-5} to 1.8×10^{-6}.

In the second period, the background radius ranges from 4.8×10^{-4} m to 4.8×10^{-3} m to 4.8×10^{-4} m, and the background content ranges from 1.6×10^{-6} to 4.8×10^{-5} to 1.6×10^{-6}.

In the third period, the background radius ranges from 5.0×10^{-4} m to 5.0×10^{-3} m to 5.0×10^{-4} m, and the background content ranges from 1.5×10^{-6} to 5.0×10^{-5} to 1.5×10^{-6}.

Considering the shallower seawater depth, the pressure decreases, the bubble radius increases and the content also increases, accompanied by the bubble breaking into small bubbles. The bubble numbers change, and thus the starting and ending values of the background radius and content in the three periods are different and generally become smaller in order.

4 Improved plume seismic records of shot gather

The plume water body model in Fig. 3 was forward simulated by a finite difference solving two dimensional acoustic wave equations. The acquisition parameters are as follows: the survey line is 3 500 m long and 1 600 m deep; the grid subdivision is 1 m×1 m; and the dominant frequency of seismic wavelet is 145 Hz. Because the seismic response is not obvious when the source frequency is low, the main frequency of the source is 145 Hz in this model. The observation system is as follows: seismic waves are received in all arrays; the array is fixed and the shot point moves; the excitation is from left to right; the shot interval is 20 m, and there are 166 shots in total; the seismic source is 20 m in depth; the trace interval is 1 m, and there are a total of 3 500 traces; the array length is 3 600 m; the least offset is zero; the record length is 3 000 ms; and the sampling rate is 0.328 ms. We sorted the 83th shot of seismic records (Fig. 4).

The seismic records in Fig. 4 are similar to Fig. 4 in reference (Li et al., 2013), and we can see that the seismic wave field also has obvious scattered wave field characteristics in the plume. The seismic records of single shot have the following features.

First, the energy features are: the scattered wave energy is strongest where the plume is; the energy weakens gradually towards two sides and rapidly upward and downward; and where the radii and the number of bubbles are larger, the energy will be stronger.

Second, the waveform features are: where there are bubbles, the seismic waveform is the scattered waves with the bubbles'

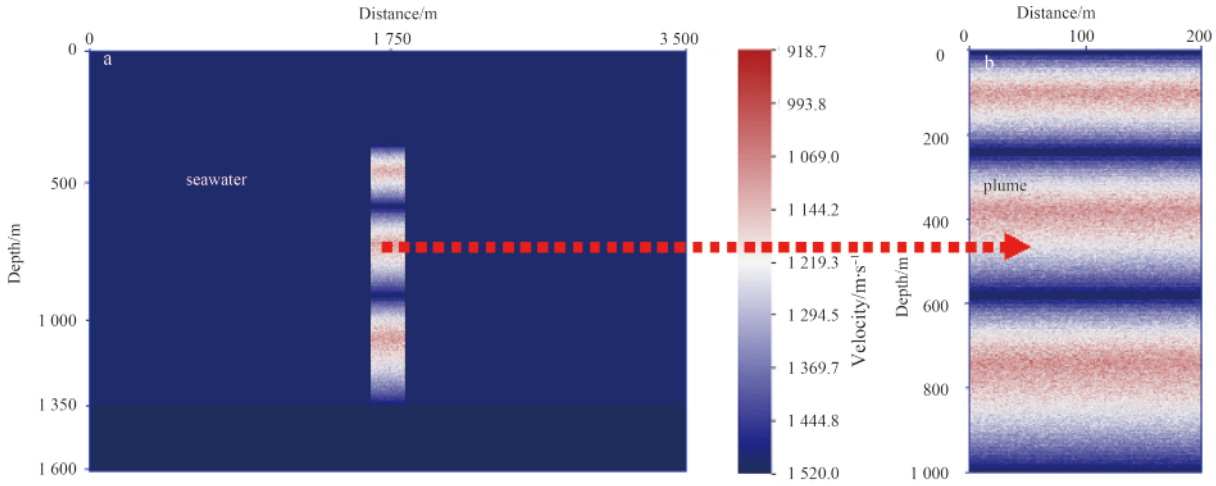

Fig. 3. A plume water body model. a. The sea water and plume, and b. a plume.

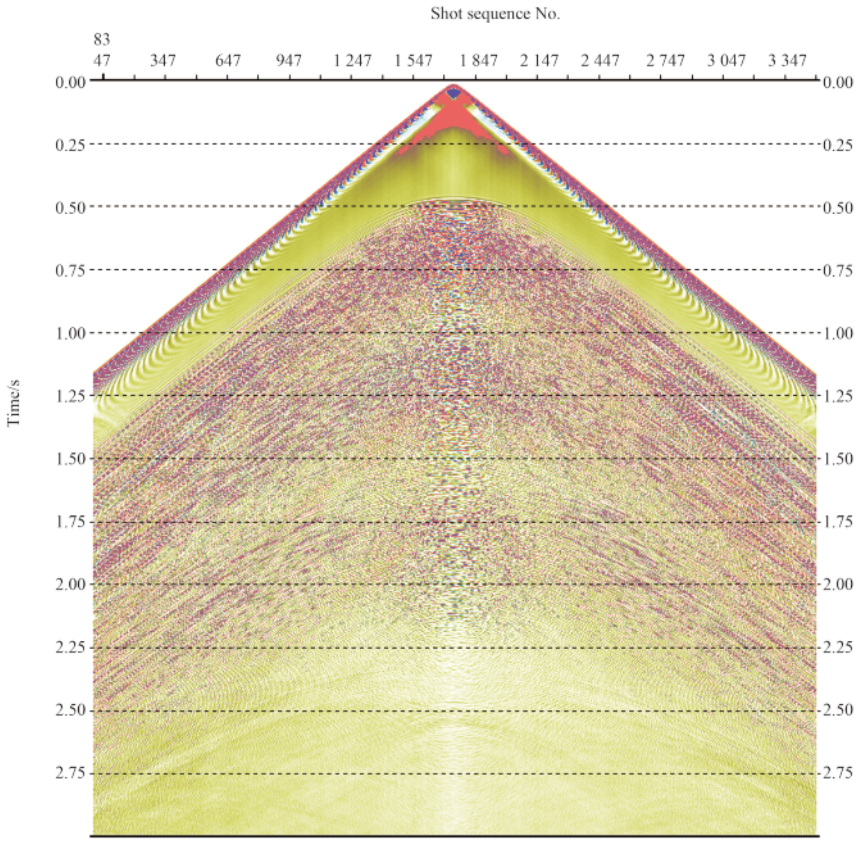

Fig. 4. The seismic records from the 83th shot gather of plume model.

location as the scattering vertex; and the coherence increases where the bubble density is high.

Third, the period characteristics are: the difference with Fig. 4 in reference (Li et al., 2013) is that shot gather records (Fig. 4) show periodic characteristics of the model (Fig. 3) and the features are more obvious for plumes in the middle position of the shot gather records. The energy of the three periods gradually weakened from top to bottom, and this is due to the effect of the difference in the geometric diffusion and model parameters (radius or content).

In the shot gather records (Fig. 4), the scattered wave field characteristics of the plume are in accordance with Yin's conclusion (Yin, 2005) on that of heterogeneous medium models. This illustrates that macroscopic manifestations of the random medium of the plume with local distribution are the same as that of a heterogeneous medium. At the same time, these characteristics correspond to the manifestations of fluctuations in the plume area (Fig. 2b). In other words, the scattered wave energy is strong where a bubble plume occurs, whereas the energy is weak in other areas. Moreover, the strength of the scattered wave energy in the plume area is related to the magnitude of the bubble radii and content. The above analytical conclusions provide a theoretical reference for identifying hydrate bubble plumes by scattered waves.

5 Improved plume prestack depth migration section

The shot gather seismic records of the original model in reference (Li et al., 2013) have obtained better migration results by using prestack time migration processing, but there is still interference energy that results in poor boundary convergence. Therefore, the shot gather seismic records of the improved model in this paper are processed by prestack depth migration (Liu et al., 2013; Zhang and Zhang, 2011) and a good imaging effect was obtained. The seismic section of the prestack depth migration is obtained and is shown in Fig. 5.

By comparing the plume model (Fig. 3) with its migration section (Fig. 5), we can draw the following conclusions.

First, the scattered waves of the plume can be imaged distinctly, and the effect of boundary convergence is better.

Second, the plume lies in the model, and its range is from 350 to 1 350 m vertically and from 1 650 to 1 850 m horizontally. The plume lies on the seismic section, and its range is from 350 to 1 350 m vertically and from 1 650 to 1 850 m horizontally. The imaging accuracy is higher.

Third, on the seismic section, stronger energy in the middle of plume in every period corresponds to a larger bubble radius and a higher bubble content in the given model.

Fourth, the period characteristics of the model (Fig. 3) can be imaged more accurately, and the imaging effect of the first period is better than that of second and third periods.

Fifth, the plume water body model can be imaged more accurately using prestack depth migration, yet when the velocity disturbance of the layers of the model is greater, the scattered waves are difficult to flatten and the energy convergence is not good.

The above improved plume water body model can be imaged more accurately by prestack depth migration, and the processing method of plume seismic data provided a theoretical guidance for identifying the bubble plume by scattering imaging. The stud-

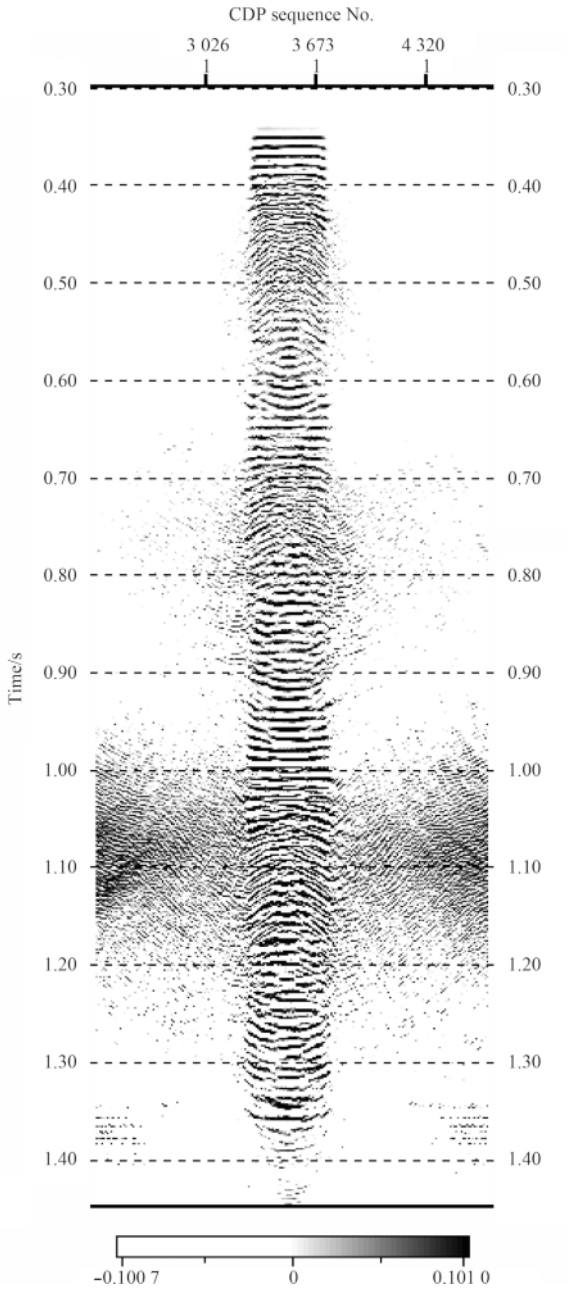

Fig. 5. A prestack depth migration section of the plume.

ies laid a foundation for further study of the seismic responses produced by plumes.

6 Conclusions

Based on the analysis of the characteristics of the water body containing bubbles at home and abroad, this paper improved the established gas hydrate plume model, and forward and inverse modelling research on the plume was carried out, with the following conclusions and understandings reached.

First, the plume water body model established by using improved ideas can better reflect the distribution of bubbles in the actual plume water body.

Second, the improved plume water body, in addition to having wave field characteristics of the original model (where the plume is, the seismic wave field has obvious scattered wave field characteristics and the energy is strongest, and in the areas where the scattered wave energy is stronger, the minimum travel time is always above the plume, which has no relationship with the shot's position), also has a periodic feature; the shot gathers that have shot in the middle position is especially obvious, and the energy of three periods gradually weakened from top to bottom.

Third, the prestack depth migration section shows that the scattered waves of the plume can be imaged distinctly. The imaging on the top of plume is better than that on the bottom, and the effect of boundary convergence is better. The periodic characteristic is obvious and the imaging accuracy is higher.

Through this study, the plume modelling scheme is more reasonable, and a more suitable seismic data processing method for plumes is also gradually explored. The study results laid a foundation for further study on the seismic responses produced by plumes and provided a theoretical reference for identifying bubble plumes by scattered wave imaging. It also provided a new approach for the identification of gas hydrates and the study of changes in the marine environment.

Acknowledgements

The authors thank Liu Xuewei of China University of Geosciences (Beijing) for providing the seismic migration section (Fig. 2a) and the bubble plumes migration section (Fig. 2b) of some areas in the South China Sea.

References

Bayon B, Birot D, Ruffine L, et al. 2011. Evidence for intense REE scavenging at cold seeps from the Niger Delta margin. Earth and Planetary Science Letters, 312(3–4): 443–452

Charlou J L, Donval J P, Zitter T, et al. 2003. Evidence of methane venting and geochemistry of brines on mud volcanoes of the eastern Mediterranean Sea. Deep Sea Research I: Oceanographic Research Papers, 50(8): 941–958

Di Pengfei, Feng Dong, Gao Libao, et al. 2008. In situ measurement of fluid flow and signatures of seep activity at marine seep sites. Prog Geophys (in Chinese), 23(5): 1592–1602

Di Pengfei, Huang Huagu, Chen Duofu. 2010. Total sulfur and calcium contents of seep fluids and their controls in the cold seep sites. Geoscience (in Chinese), 24(3): 570–575, 580

Fan Shuanshi, Liu Feng, Chen Duofu. 2004. The research of the origin mechanism of marine gas hydrate. Nat Gas Geosci (in Chinese), 15(5): 524–530

Freire A F M, Matsumoto R, Santos L A. 2011. Structural-stratigraphic control on the Umitaka Spur gas hydrates of Joetsu Basin in the eastern margin of Japan Sea. Marine and Petroleum Geology, 28(10): 1967–1978

Gong J M. 2006. Methane plumes on marine gas hydrate ore reservoir in the east edge of Japan Sea-the possible mechanism of ground methane transporting to the shallow water. Mar Geol Lett (in Chinese), 22: 33

Greinert J, Artemov Y, Egorov V, et al. 2006. 1300-m-high rising bubbles from mud volcanoes at 2080 m in the Black Sea: Hydroacoustic characteristics and temporal variability. Earth and Planetary Science Letters, 244(1–2): 1–15

Hao Zhaobing, Huang Weiqing, Qin Jingxin, et al. 2013. Estimation technique for gas hydrate saturation of pressure core samples. Chinese J Geophys (in Chinese), 56(11): 3917–3921

Heeschen K U, Tréhu A M, Collier R W, et al. 2003. Distribution and height of methane bubble plumes on the Cascadia Margin characterized by acoustic imaging. Geophysical Researcher Letters, 30(12): 1643

Holbrook W S, Páramo P, Pearse S, et al. 2003. Thermohaline fine structure in an oceanographic front from seismic reflection profiling. Science, 301(5634): 821–824

Hu Lei, Yvon-Lewis S A, Kessler J D, et al. 2012. Methane fluxes to the atmosphere from deepwater hydrocarbon seeps in the north-

ern Gulf of Mexico. Journal of Geophysical Research Oceans, 117(C1): 92–99

Ju Hua, Chen Gang, Li Guodong. 2011. Research on numerical simulation of motion behaviors of single bubble rising in still water. Journal of Xi'an University of Technology (in Chinese), 27(3): 344–349

Klaucke I, Weinrebe W, Petersen C J, et al. 2010. Temporal variability of gas seeps offshore New Zealand: Multi-frequency geoacoustic imaging of the Wairarapa area, Hikurangi margin. Marine Geology, 272(1–4): 49–58

Kvenvolden K A. 1993. Gas hydrates as a potential energy resource: a review of their methane content. In: Howell D G, ed. The Future of Energy Gases-US Geological Survey Professional Paper 1570. Washington: United States Government Printing Office, 555–561

Kvenvolden K A, Ginsburg G D, Soloviev V A. 1993. Worldwide distribution of subaquatic gas hydrates. Geo-Mar Lett, 13(1): 32–40

Li Canping, Liu Xuewei, Gou Limin, et al. 2013. Numerical simulation of bubble plumes in overlying water of gas hydrate in the cold seepage active region. Science China: Earth Sciences, 56(4): 579–587

Liu Bosheng, Liu Jiayu. 2010. The Principle of Acoustics. 2nd ed. Harbin: Harbin Engineering University Press (in Chinese), 6–15

Liu Haijun, An Yu. 2004. Pressure distribution outside a single cavitation bubble. Acta Physica Sinica(in Chinese), 53(5): 1406–1412

Liu Linong, Zhang Hui, Zhang Jianfeng. 2013. Angle gathers for one-way wave equation shot-record migration methods. Chinese J Geophys (in Chinese), 56(9): 3124–3133

Lu Zhenquan, He Jiaxiong, Jin Chunshuang, et al. 2013. A study of modeling the effects of gas sources on gas hydrate formation in the northern slope of South China Sea. Chinese J Geophys (in Chinese), 56(1): 188–194

Luan Xiwu, Liu Hong, Yue Baojing, et al. 2010. Characteristics of cold seepage on side scan sonar sonogram. Geoscience (in Chinese), 24(3): 474–480

MacDonald I R, Bender L C, Vardaro M, et al. 2005. Thermal and visual time-series at a seafloor gas hydrate deposit on the Gulf of Mexico slope. Earth and Planetary Science Letters, 233(1–2): 45–59

Pinheiro L M, Song H B, Ruddick B, et al. 2010. Detailed 2-D imaging of the Mediterranean outflow and meddies off W Iberia from multichannel seismic data. Journal of Marine Systems, 79(1–2): 89–100

Sassen R, Losh S L, Cathles III L, et al. 2001. Massive vein-filling gas hydrate: relation to ongoing gas migration from the deep subsurface in the Gulf of Mexico. Marine and Petroleum Geology, 18(5): 551–560

Sauter E J, Muyakshin S I, Charlou J L, et al. 2006. Methane discharge from a deep-sea submarine mud volcano into the upper water column by gas hydrate-coated methane bubbles. Earth and Planetary Science Letters, 243(3–4): 354–365

Shipboard Scientific Party. 2002. Ocean Drilling Program, Leg 204 Preliminary Report. Drilling Gas Hydrates on Hydrate Ridge, Cascadia Continental Margin, 7 July–2 September 2002, Texas A&M University, 1000 Discovery Drive, College Station TX 77845–9547, USA December 2002.

Tryon M D, Brown K M, Torres M E. 2002. Fluid and chemical flux in and out of sediments hosting methane hydrate deposits on Hydrate Ridge, OR, II: Hydrological processes. Earth and Planetary Science Letters, 201(3–4): 541–557

Tryon M D, Brown K M. 2004. Fluid and chemical cycling at Bush Hill: Implications for gas-and hydrate-rich environments. Geochemistry, Geophysics, Geosystems, 5(12): 1–7

Wang Xiujuan, Wu Shiguo, Wang Jiliang, et al. 2013. Anomalous wireline logging data caused by gas hydrate dissociation in the Shenhu area, northern slope of South China Sea. Chinese J Geophys (in Chinese), 56(8): 2799–2807

Wu Rushan, Aki K. 1993. In: Li Yuche, Lu Shoude, Trans. Scattering and Attenuation of Seismic Waves (in Chinese). Beijing: Seismic Press, 1–5

Xu Mairong, Liu Chengyun. 2008. The change of radius and velocity of the rising bubble in water. College Physics (in Chinese), 27(11): 14–17

Yao Wenwei. 2008. Effect of bubble on propagation of acoustic wave. Journal of Shaanxi Institute of Education (in Chinese), 24(1): 107–109

Yin Junjie. 2005. A study on seismic scattered wave characteristics by numerical simulating [dissertation] (in Chinese). Beijing: China University of Geosciences (Beijing), 23–129

Zhang Jiangjie, Zhang Jianfeng. 2011. Wave equation based migration velocity estimation: a direct inversion approach. Chinese J Geophys (in Chinese), 54(3): 835–844

Zhang Yongqin. 2010. Exploration current status of the gas hydrate abroad and the progress of the gas hydrate in China. Exploration Engineering (in Chinese), 37(10): 1–8